Anisotropy effects on gigacycle fatigue behaviour of high Cr alloyed cold work tool steel

Ch. R. Sohar[1], A. Betzwar-Kotas[2], Ch. Gierl[1], B. Weiss[2], H. Danninger[1]*

[1] *Institute of Chemical Technologies and Analytics, Vienna University of Technology, Getreidemarkt 9/164-CT, A-1060 Vienna, Austria*
[2] *Nanostructured Materials – Micromaterials, Faculty of Physics, University of Vienna, Vienna, Austria*

Received 13 December 2007, received in revised form 15 July 2008, accepted 21 July 2008

Abstract

Gigacycle fatigue behaviour of wrought cold work tool steel of AISI D2 type (DIN Nr. 1.2379) was studied employing an ultrasonic fatigue testing system operating under fully-reversed tension-compression mode ($R = -1$) at 20 kHz up to $N_{max} = 10^{10}$. The work presented here focused on the effect of anisotropy on the material fatigue behaviour. Primary carbides (clusters) located near/at the surface were found to be fatigue crack initiation sites. Fracture surfaces revealed rather flat surface morphology and around the crack origin half of so-called fish-eye was obtained. A granular area (GA) was observed surrounding the carbide particles, followed by a very flat zone. The obtained *S-N* data showed considerable anisotropy of the fatigue behaviour. Specimens with their axis perpendicular to the rolling direction revealed about 150 MPa lower fatigue endurance strength at 10^{10} loading cycles compared to samples with axis parallel to the rolling direction. Detailed investigation of fracture surface was performed in order to evaluate fatigue crack nucleation and propagation.

K e y w o r d s: tool steels, gigacycle fatigue, material anisotropy, carbide clusters, ultrasonic fatigue testing

1. Introduction

Medium-carbon high-chromium cold work tool steels (DIN 1.2379/AISI D2) are widely used in cold work applications such as blanking, forming, (powder) pressing, and stamping processes, benefiting from the high wear resistance and compressive strength provided by the numerous primary alloy carbides. During service operations, tools are repeatedly exposed to stresses and strains due to the contact between tool and workpiece. These stresses are rarely of uniaxial nature. Failure of the tool might occur as a consequence of wear, which represent the majority of service failure, but also fatigue failure of the tool material [1] might take place. Due to the frequently multiaxial loading of the tool, material anisotropy might play a decisive role for the tool life. Cast, forged and rolled materials generally reveal oriented mechanical properties due to anisotropy of the material microstructure that can be e.g. crystallographic textures, elongated grain structure, or orientation of additional phases such as alloy carbides or non-metallic inclusions. The tool steel studied here (AISI D2 type) is conventionally cast and hot worked variant containing numerous primary chromium carbides that offer high hardness and thus are responsible for high abrasion resistance of the material. However, these hard phases are elongated in the rolling direction during hot working. Thus, anisotropy of the mechanical properties of this tool steel can be expected, which should hold also for the fatigue behaviour of the tool steel.

However, investigations [2–8] of fatigue behaviour of tool steels, especially in the gigacycle regime, are scarce, which is in contrast to high strength steels, such as bearing and spring steels, for which numerous studies exist [8, 9]. Berns et al. [2] were among the first who investigated fatigue fracture of tool steels, although N_{max} was limited to 10^6 loading cycles. In rotating bending and compact tension tests of AISI D2 type tool steel, those authors found that fatigue cracks definitely started at the edges of primary chromium carbides or at fractured carbide particles. Fukaura et

*Corresponding author: tel.: +43 1 58801 16134; fax: +43 1 58801 16199; e-mail address: hdanning@mail.tuwien.ac.at

Table 1. Chemical composition of studied tool steel (obtained by X-ray fluorescence; carbon content taken out of Böhler data sheet)

Steel	AISI symbol	Chemical composition (weight percentage)							
		C	Si	Mn	Cr	Mo	V	W	Co
X155 CrVMo 12.1	D2	1.55	0.32	0.32	12.7	0.85	0.89	0.12	0.12

al. [4], who tested a JIS-SKD 11 (AISI D2 type equivalent) tool steel in a rotating bending system up to 10^7 cycles, also found primary chromium carbides as nucleation sites for fatigue cracks. At stress amplitudes above about 1000 MPa, fatigue cracks originated at carbide particles located at the surface, and at lower stress amplitudes so-called internal "fish-eye" type failure at internal carbide particles was observed [4]. Berns et al. [3] compared the fatigue behaviour of powder metallurgically (PM) and conventionally produced high speed steels up to $N_{\max} = 10^6$. While in vacuum sintered PM steels, cracks started at pores and, after hot working, at nonmetallic inclusions mostly in the subsurface region, in conventional steel the primary alloy carbides located in the surface layer gave rise to fatigue cracks, since they represent the largest discontinuity within the material and have a high frequency of occurrence. The present authors showed earlier [8] that primary carbide particles or clusters located at/near the surface or – if compressive residual stresses existed at the specimen surface – in the interior of the specimen initiate fatigue cracks in the gigacycle fatigue regime. Since primary carbides definitely can nucleate fatigue cracks, any anisotropic distribution of these carbides in the steel might significantly affect the fatigue behaviour, which has not been studied for tool steels until now. In bearing and spring steels, for which the occurrence of non-metallic inclusions is decisive for fatigue behaviour of the material, recent investigations revealed a strong influence of material anisotropy. Furuya et al. [10] showed for 1800 MPa-class spring steels that differences of fatigue strength were insignificant for specimens prepared from bars with different degree of deformation, which was attributed to the fact that effective inclusions were of similar small size in both cases. However, specimens with axis transverse to the rolling direction revealed significantly reduced fatigue strength [10] – about 50 % of those in the rolling direction. This effect is due to large, elongated MnS inclusions – definitely a fatigue anisotropy effect. Transverse specimen from bars with lower degree of deformation showed worse fatigue behaviour due to larger inclusions. Temmel et al. [11] recently observed a similar influence of MnS inclusions on the fatigue behaviour for low-alloyed structural steel (42CrMo4). Steel variants with high sulfur content revealed more pronounced anisotropy, which was attributed to the higher MnS population. Kaynak et al. [12] observed strongly anisotropic behaviour of short cracks in Mn alloyed mild steel En7A with high content of elongated MnS inclusion.

The goal of the present study was to evaluate the effect of anisotropy on the gigacycle fatigue behaviour of a wrought medium-carbon high-chromium tool steel (AISI D2 type). For this material not MnS inclusions, but alloy carbides are responsible for the material anisotropy. Employing a 20 kHz ultrasonic resonance fatigue testing system offered the advantage of reliable results in the gigacycle range at acceptable times and costs. This study was aimed to provide new results in area of gigacycle fatigue behaviour of very hard materials, especially of tool steels, for which knowledge is currently limited.

2. Experimental

The steel studied in this work was a wrought cold work tool steel 1.2379, acquired from *Böhler Edelstahl GmbH*, Austria (Böhler grade K110), in annealed condition as cylindrical bars with a diameter of 15.5 mm (bar "B1", strongly hot worked) and 106 mm (bar "B2", moderately hot worked). Chemical composition as derived from X-ray fluorescence analysis is shown for the major constituents in Table 1. Fatigue tests of five different specimen test series were performed: In order to evaluate anisotropic properties of conventionally produced steels, specimens were prepared with their axis in rolling direction (K110LL-M, K110LL-A) and orthogonal to the rolling direction (K110TT-M, K110TT-A). Specimens designated with "M", were machined from the inner core of the 106 mm bar and specimens "A" from "outside" were distinguished, as shown in Fig. 1. Furthermore, longitudinal specimens (K110L) were also prepared from the more strongly hot worked cylindrical bar "B1" in order to study probable effect of the degree of hot rolling deformation. All specimens were turned to the desired geometry [8] and their surface longitudinally ground prior to the heat treatment in such a way that the specimen slowly rotated while polished by a rapidly rotating disk parallel to specimen axis. The rotating disk was spring mounted in order to avoid undesired pressure on the sample, which might induce stresses in the material. The steel was then austenitized at 1040 °C for 25 min and quenched in oil. Tem-

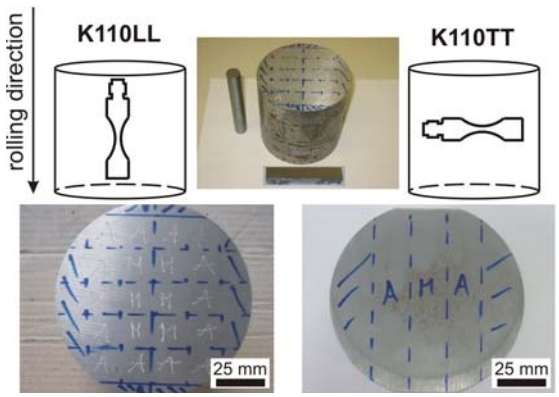

Fig. 1. Orientation of fatigue specimens in the steel bar.

pering was done at 530 ℃ for 2 hrs. All heat treatments were performed under high purity nitrogen atmosphere (5.0 N_2). Relatively high tempering temperature and slow subsequent cooling was chosen in order to reduce the amount of retained austenite, to lower quench-induced residual stresses and minimize thermal stresses in the workpiece, respectively. The heat treated hour glass shaped fatigue specimens were then polished to mirror-like finish in the longitudinal direction using 240 mesh alumina oxide abrasive paper, 15 μm and 6 μm diamond suspension, similar to the grinding accomplished before the heat treatment as described above. Polishing using 15 μm diamond suspension was applied for material removal in order to eliminate grinding-induced surface compressive residual stresses (RS), up to 150 μm being removed (see also 3.1). Devices used for the determination of mechanical properties have been presented earlier [8], which holds also for the applied etching reagents to reveal steel microstructure. Residual stresses have been measured at the surface in the narrowest section of the fatigue samples, employing X-ray diffraction and the $\sin^2\Psi$-method [Cr Kα, $\theta = 78.06°$, lattice plane: {211}, $^1/_2S_2 = 6.09 \times 10^{-6}$]. For fatigue testing an ultrasonic testing system (*Telsonic-Ultrasonics*, Switzerland) operating at 20 kHz in fully reversed mode ($R = -1$) was employed, of which details have been presented recently [8]. The probability of cavitation and corrosion due to the specimen cooling, which was required due to the heat developed within the samples during fatigue testing, was intensively discussed in previous work [8]; it was concluded that these effects are negligible. Fracture surfaces were examined by means of scanning electron microscopy.

3. Results and discussion

3.1. Material characterization

After the applied heat treatment, uniform fine-structured tempered martensite was obtained, indicating that only a low amount of retained austenite was present after tempering at high temperature. XRD proved that the amount of retained austenite was a few percent maximum. Prior austenite grain sizes have been examined in the as-quenched structure employing the Snyder-Graff method. They turned out to be 13 ± 2 μm for the heat treatment applied here. Figure 2 shows light optical micrographs of the microstructure after the applied heat treatment in the transverse and longitudinal section for both bars. Samples were etched with Murakami's reagent that colours the chromium carbides. The transverse carbide distribution is rather uniform, which holds for both bars (compare Fig. 2a,b). Visually, carbides (clusters) seem to be somewhat larger in bar B2 compared to bar B1, supposedly due to the lower degree of deformation of bar B2. In the longitudinal sections (Fig. 2b,d) the primary carbide bands were observed as characteristic for cast and rolled tool steel. The carbide bands are broader in bar B2 compared to bar B1, and carbide clusters are smaller in bar B1. Obviously, the carbide clusters are significantly larger in the longitudinal direction compared to the transverse direction, which can be seen quite well in the optical micrographs at 500× magnification (Fig. 2e,f). A rough classification of the primary carbides (clusters) after their diameters was performed using 10 to 12 optical micrographs at magnification 200× for both orientations. Results are presented in Table 2. The largest species of carbide clusters in the transverse section had diameters of about 60 and 100 μm in bar B1 and B2, respectively. Larger elongated species were observed at higher frequency of occurrence in the longitudinal direction of the steel. Again, more of the largest species were observed in samples of bar B2. Consequently, a strong anisotropy of the mechanical properties can be expected, which was indeed proved by the strong orientation dependence of the transverse rupture strength (T. R. S.), as shown in Table 3 (compare results of LL to TT). Not surprisingly, the dynamic Young's modulus and material hardness did not reveal such a relationship. The primary carbides were identified as alloy carbides of type $(Fe,Cr)_7C_3$ by means of XRD. The volume fraction was determined by image analysis of 25 optical images at 500× and 1000× magnification, and it turned out to be 12 ± 1 %, which was similar to results found by Fukaura et al. [4]. It should be noted that non-metallic inclusions have not been detected in metallographic sections. Furthermore, residual stresses at the specimen surface were determined by means of XRD. It was found [8] that high surface residual stresses were introduced through grinding after the heat treatment process. In order to eliminate these stresses, polishing of the specimens with 15 μm diamond suspension was performed. This procedure resulted in surface stresses in the range of +40

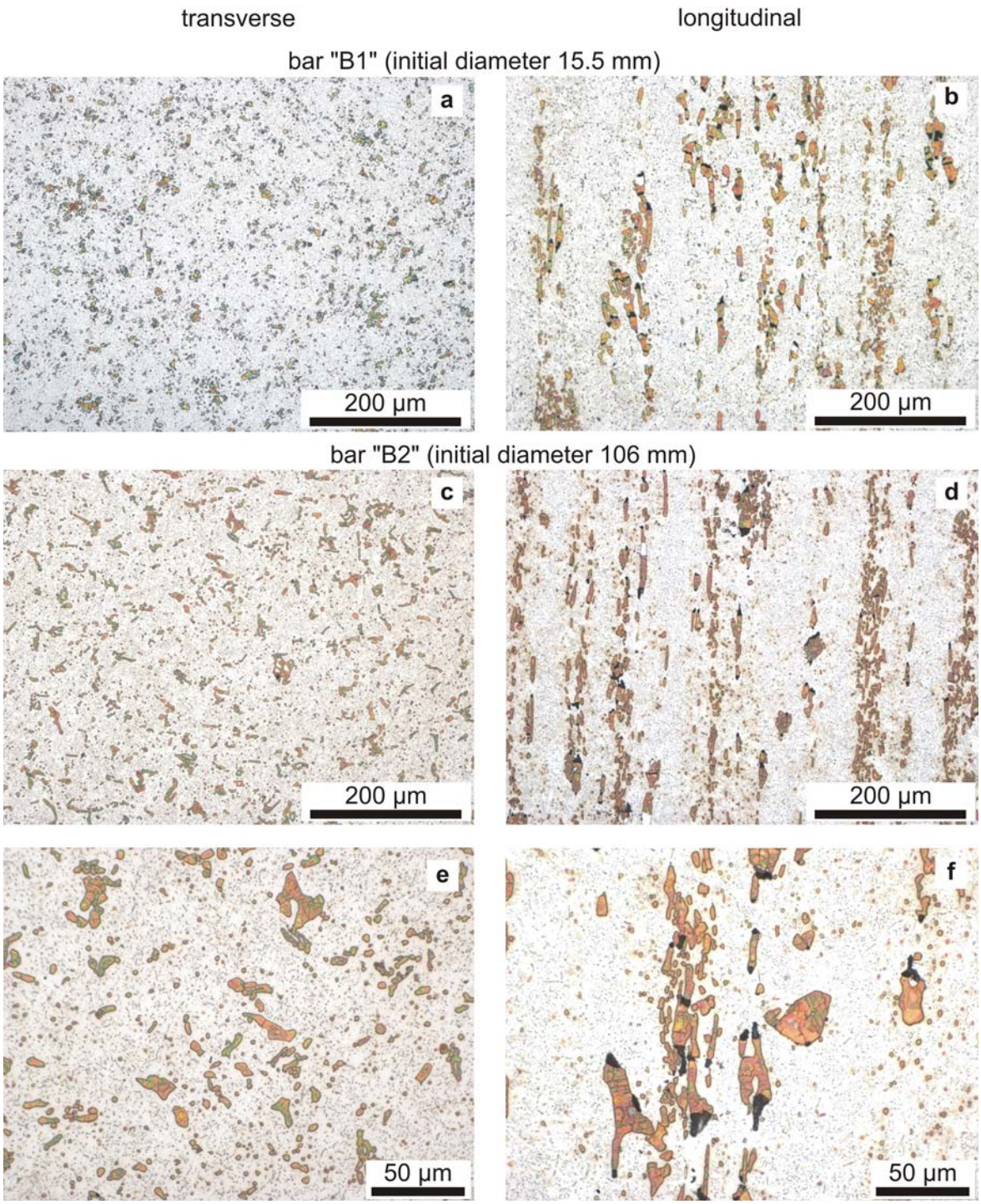

Fig. 2. Optical micrographs of as-heat treated microstructure of AISI D2 type tool steel.

to −195 MPa for K110LL and K110L specimens, for which material removal down to a depth 40 to 60 µm was performed. However, it turned out that in case of K110TT specimens the surface RS existing after the polishing were between −195 and −340 MPa, despite material removal to a depth of 150 µm. This can probably be attributed to different wear behaviour in that direction of the material due to the alignment of the primary carbide bands. This fact has to be considered when interpreting the fatigue data.

3.2. Fatigue data

Figure 3 presents the *S-N* curves for the two test series K110LL and K110TT. The fatigue data obviously revealed a strongly anisotropic gigacycle fatigue

Table 2. Classification of carbides according to their sizes as found in metallographic sections

Carbide (cluster) diameters (μm)	Relative frequency (%)			
	bar B1		bar B2	
	transversal	longitudinal	transversal	longitudinal
20	74	68	57	not determined
40	21	19	25	36
50	4	6	10	26
60	1	6	5	18
80	0	1	2	13
100	0	0	1	6

Table 3. Measured mechanical properties of the studied steel; confidence interval 95 %

Steel "K110" AISI D2 1.2379	Rockwell hardness HRC 150 kg		Microhardness HV 25 g		T. R. S. (MPa)	Dynamic Young's modulus (GPa)
	as-quenched	tempered	matrix	alloy carbides	tempered steel	tempered steel
K110L (parallel to RD)	64 ± 1	58 ± 2			3600 ± 350	210 ± 7
K110LL (parallel to RD)	64 ± 1	59 ± 1	755 ± 30	1540 ± 215	3900 ± 300	205 ± 6
K110TT (perpendicular to RD)	62 ± 2	58 ± 1			1950 ± 150	209 ± 10

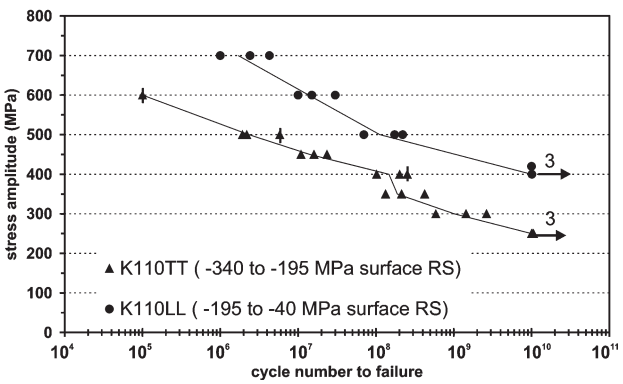

Fig. 3. *S-N* curves of test series K110LL and TT of AISI D2 tool steel.

behaviour of the steel. K110TT (Fig. 3▲) specimens showed significantly lower fatigue strength over the entire tested fatigue life range compared to K110LL specimens (Fig. 3●). It is noted that the somewhat higher compressive residual stresses – present at the surface of K110TT specimens – have to be considered in this respect. This means that theoretically, K110TT specimens with RS similar to K110LL specimens are expected to show even lower fatigue strength than the experimental results observed here. Crack initiation sites were closely-spaced primary carbides, referred to as carbide clusters, or in some few cases large primary carbides. These defects were located at/near the surface (Fig. 4). Interestingly, more near-surface crack origins were observed for K110TT specimens. Carbides were always found to be cracked, i.e. initiation through cracking of larger carbides is dominant here compared to carbide-matrix decohesion. Some K110TT specimens failed due to surface cracks. The lower fatigue strength of K110TT specimens compared to the K110LL specimens can be attributed to the considerably higher frequency of occurrence of the large carbide clusters (80 to 100 μm diameter) in the longitudinal direction of the steel (bar B2) – which corresponds to the fracture area of K110TT samples (Table 2). The diameters of carbide clusters, which gave rise to fatigue cracks in K110TT specimens, ranged from 56 to 172 μm. In K110LL specimens far smaller carbide clusters (10 to 48 μm in diameter) were found to be crack origins. This is reflected by the higher fatigue strength in the *S-N* data of the K110LL test series (Fig. 3●). At this point it should be mentioned that no difference of the fatigue behaviour was obtained between samples from the inner core (samples "M") and from the "outer part" (samples "A") of the bar B2. This means that the distribution of primary carbides seemed to be very homogeneous within the steel bar.

Furthermore, the degree of deformation did not have an impact on the fatigue behaviour of the studied AISI D2 type tool steel either, at least with specimens oriented parallel to the rolling direction. Specimens of series K110LL (bar B2 – larger initial bar diameter) failed within the same cycle number ranges as specimens of the more heavily deformed series K110L (bar

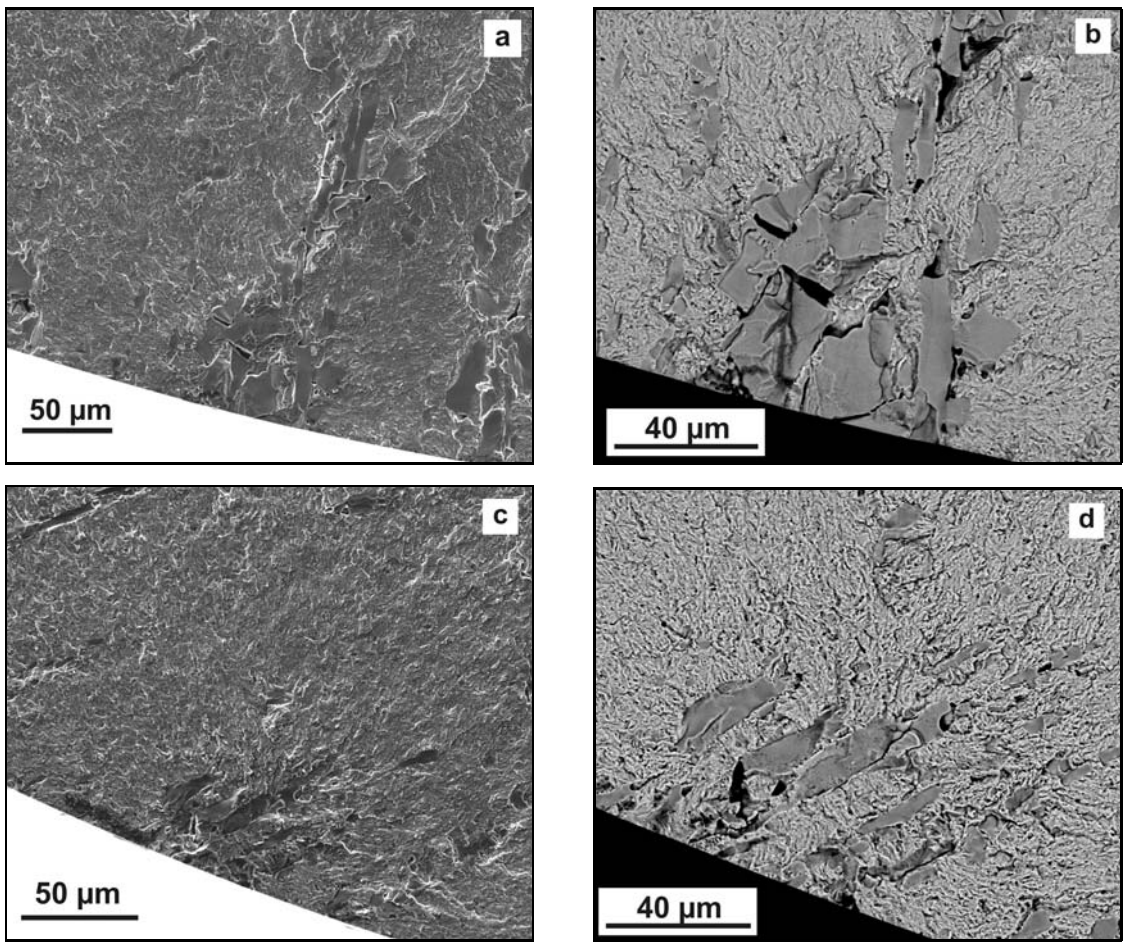

Fig. 4. Crack origins of K110TT specimens failed: (a, b) after 1.9×10^6 cycles at 500 MPa (carbide cluster touching the surface), and (c, d) after 1.3×10^8 cycles at 350 MPa (carbide cluster below the surface).

B1), results of which have been presented earlier [8]. This finding was in accordance with results obtained for the spring steel by Furuya et al. [10]. Those authors [10] claimed that differences of fatigue strength were small for specimens prepared from bars with different degree of deformation, which was attributed to the fact that effective inclusion sizes were similarly small in both cases. This holds also for the steel studied here: The maximum carbide cluster size observed in transverse metallographic section (which corresponds to the fracture area of specimens K110L and LL) of bar B2 was larger than in bar B1 (see Table 2). However, the relative frequency of these large species was rather low. Hence, the fatigue behaviour of the two test series K110L and LL was similar. Some internal fish-eye type crack initiation was observed for K110L specimens in the cycle number range 10^5 to 10^7, which is in agreement with statistical considerations [8]. However, such internal failures were not obtained for K110TT samples probably due to the high frequency of occurrence of large carbides (clusters) which makes the existence of such a large species in the surface layer – where the highest stress concentration occurs [13] – much more probable.

3.3. Fractography

In order to receive more information about the crack initiation and propagation processes in the studied tool steel, and especially to evaluate probable differences between the two sample orientations (K110TT and K110LL), the obtained fracture surface of every specimen was investigated by means of SEM. Figure 5 presents representative fractographs of the two test series K110LL (Fig. 5a,b) and K110TT (Fig. 5c,d). Obviously, a strong difference of the macroscopic appearance of the fracture surface between the two series was observed. While in K110LL fractographs numerous cracks, found at the major part of the fracture surface, point back to the fatigue crack origin (marked with an arrow in Fig. 5a), K110TT fractures exhibited a completely different picture. Here, numerous cracks oriented parallel to the primary carbide bands were observed (Fig. 5c). It is noted here that K110L and K110LL specimens revealed very sim-

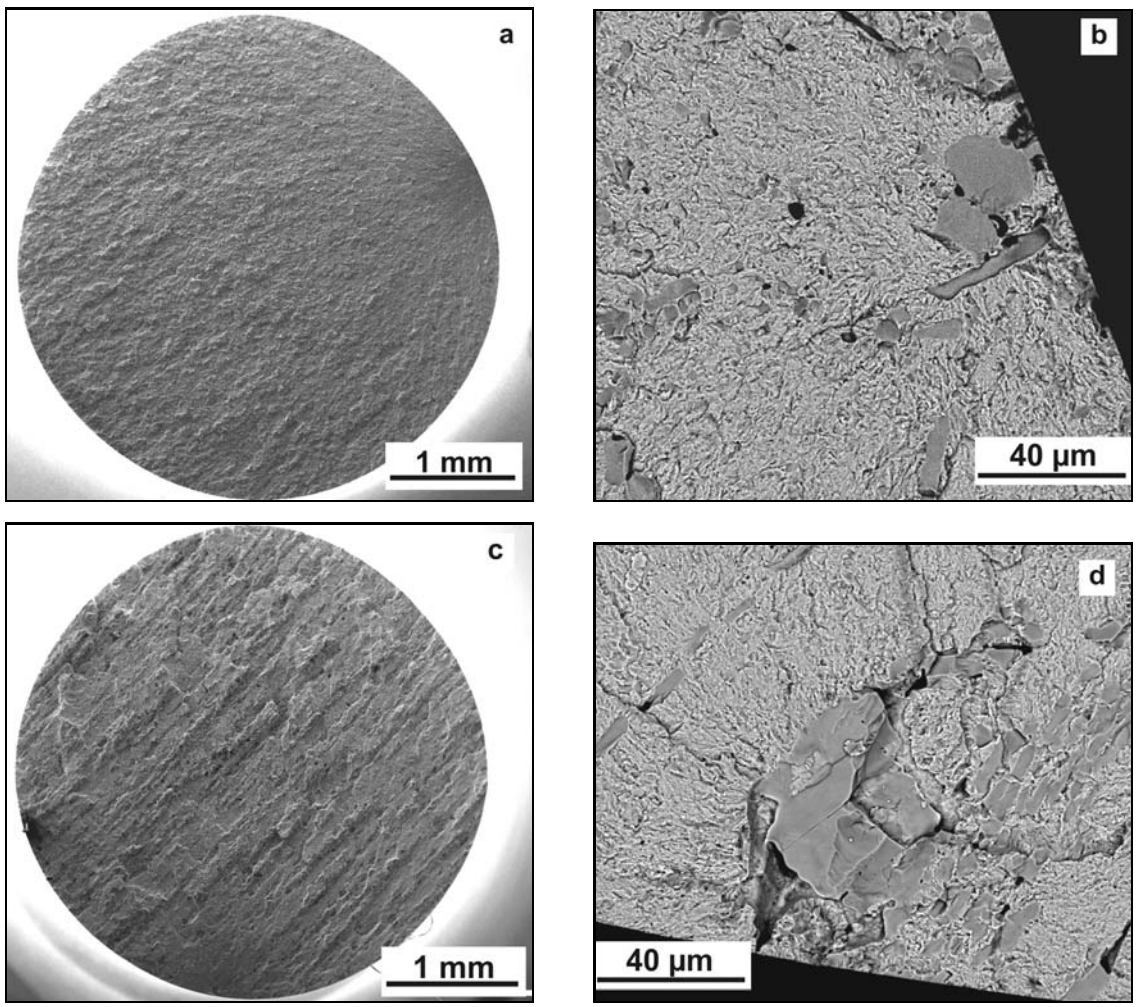

Fig. 5. Representative fractographs of specimens failed after (a, b) 1.5×10^7 cycles at 600 MPa (K110LL), and (c, d) after 1.6×10^7 cycles at 450 MPa (K110TT).

ilar fracture surface, which is in accordance with the obtained *S-N* data that did not reveal any difference of fatigue lifetime. Due to that similarity, and since K110L results have been presented earlier [8], they are not discussed here.

Around the crack origin a specific area was formed for all fractures of the three test series. This area appeared dark in SEM micrographs indicating a rather flat surface morphology. Such a dark area around the crack origin was also observed by Murakami et al. [14], who called it "optical dark area" (ODA). The similarity of the appearance of the initial stages of fatigue process for specimens LL, L and TT and the fact that for both series K110LL and K110TT carbides (clusters), just touching the surface or being located just below the surface, were nucleation point of fatigue cracks (Figs. 4 and 5 – high magnification SEM images) indicate that fatigue crack initiation and early propagation are rather similar for the two material orientations.

As mentioned before, primary carbides (clusters) were found to be nucleation point of fatigue cracks. In case of K110TT specimens (Fig. 5c,d) the crack initiating carbide clusters were far larger than those observed in K110LL samples (Fig. 5a), which directly corresponds to the larger carbide clusters sizes found in the longitudinal metallographic sections of bar B2 compared to the transverse direction (Table 2 – bar B2). Obviously, the larger carbides (clusters) are responsible for the significantly lower fatigue strength at the same sample life, as shown in the *S-N* data. This fact underlines the strong effect of the material anisotropy on the gigacycle fatigue behaviour of this AISI D2 type tool steel.

An interesting observation was made with respect to the orientation of the primary carbide bands to the specimen surface at the crack origin. For about 60 % of the failed K110TT specimens the carbide bands revealed an angle with the surface in the range between 20 and 50° (Fig. 4c,d). Only one specimen failed due to carbide bands parallel to the specimen surface (angle = 0°, Fig. 6). About one third of the failed specimen

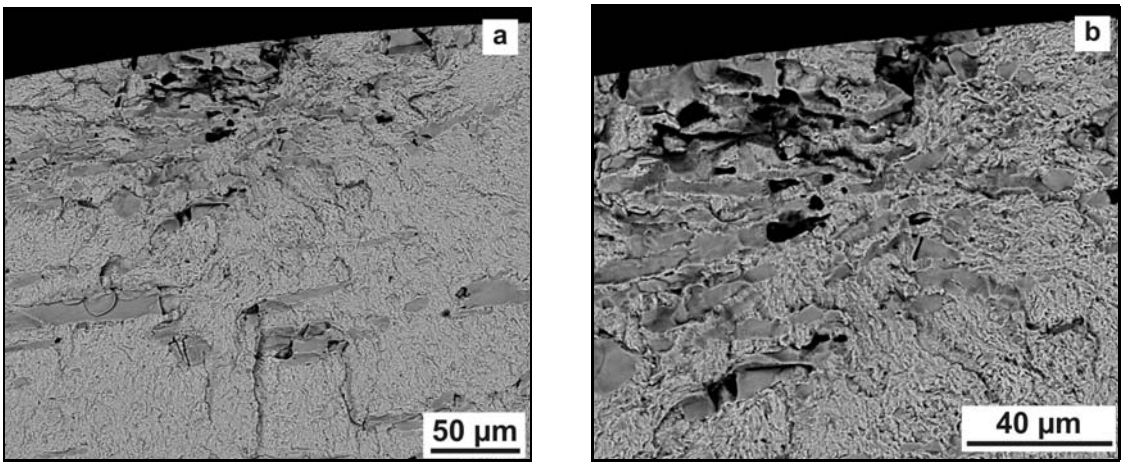

Fig. 6. Fracture surface of K110TT specimen failed after 2.6×10^9 cycles at 300 MPa; Carbide bands oriented parallel to specimen surface.

showed an angle between primary carbide bands and specimen surface of 60 to 90° (Fig. 4a,b and Fig. 5c,d). This observation is in strong contrast to K110LL specimens, for which all the fractures had more or less the same appearance.

Detailed investigations of the different zones on the obtained fracture surfaces of K110TT specimens were carried out in the way as done earlier by the authors for K110L specimens [15]. As it was noted above, K110LL and K110L fractures showed similar appearance, so that the present work focused on K110TT results. Figure 7 presents a typical zone around the crack origin of fractured K110TT specimens. Around the crack origins (carbide clusters) a granular area (GA) was observed similar to that obtained for K110L specimens [15]. This granular area (Fig. 7d) revealed a considerably roughened surface morphology compared to zone "2a" (Fig. 7c). It is speculated that the GA is formed according to a model introduced by Shiozawa et al. [16], called "dispersive decohesion of spherical carbides". The model suggests that multiple microcracks are initiated by decohesion of small carbides (diameter < 1 µm) from the iron matrix. This process of microcrack formation and subsequent coalescence of these microcracks is rather slow. Shiozawa et al. [16] claimed that most of fatigue life is spent to form an appropriate size of GA which then triggers a short fatigue crack. The border of the granular area (GA) and the area "2a" probably marks the transition from a non-propagating to a propagating fatigue crack. More precisely, the short crack, formed through coalescence of numerous microcracks within the GA, reached a crack length of a propagating crack. Before this crack length is attained, growth can only take place by microcrack coalescence. The area "2a" (Fig. 7a), also observed for K110L [15] and K110LL specimens and characterized by a rather flat surface morphology (Fig. 7c), probably represents the second stage of the fatigue failure process, corresponding to the propagation of short fatigue cracks. At fracture surfaces of K110L specimens two more crack growth zones were observed [15]. However, K110TT fractographs did not clearly exhibit such further stages of crack propagation. It seems that outside of area "2a", a zone with higher surface roughness exists that passes into the final fracture area, where numerous cracks parallel to the primary carbide bands are visible.

3.4. Fracture mechanical considerations

The diameters of the carbide clusters, the GA and of stage "2a" were evaluated in order to obtain information about the fatigue process. However, it should be considered that exact determination of the size of area "2a" was possible only with difficulties, since the transition from stage "2a" to subsequent fatigue stage was rather smooth. Figure 8a clearly shows that the lower the applied stress amplitude the larger the observed sizes of the GA and stage "2a". This means the lower the applied stress amplitude the larger is the required GA size to trigger a short crack. This observation supports the Shiozawa [16] model. The sizes of carbide clusters in the GA centre did not reveal such a relationship, neither to the stress amplitude nor to the cycle number to failure. Furthermore, the GA formation can be described numerically by the difference of the granular area size minus carbide cluster size, which is plotted against cycle number to failure in Fig. 8b. There exists a strong correlation with the specimen life. Longer fatigue life means larger granular area and larger difference of (GA minus carbide cluster size). Neither carbide cluster sizes nor sizes of the area "2a" showed any relationship to the fatigue life.

At cycle numbers below 10^7 – at high stress amplitudes – the observed GA size and carbide cluster size were rather equal, thus, the difference GA size

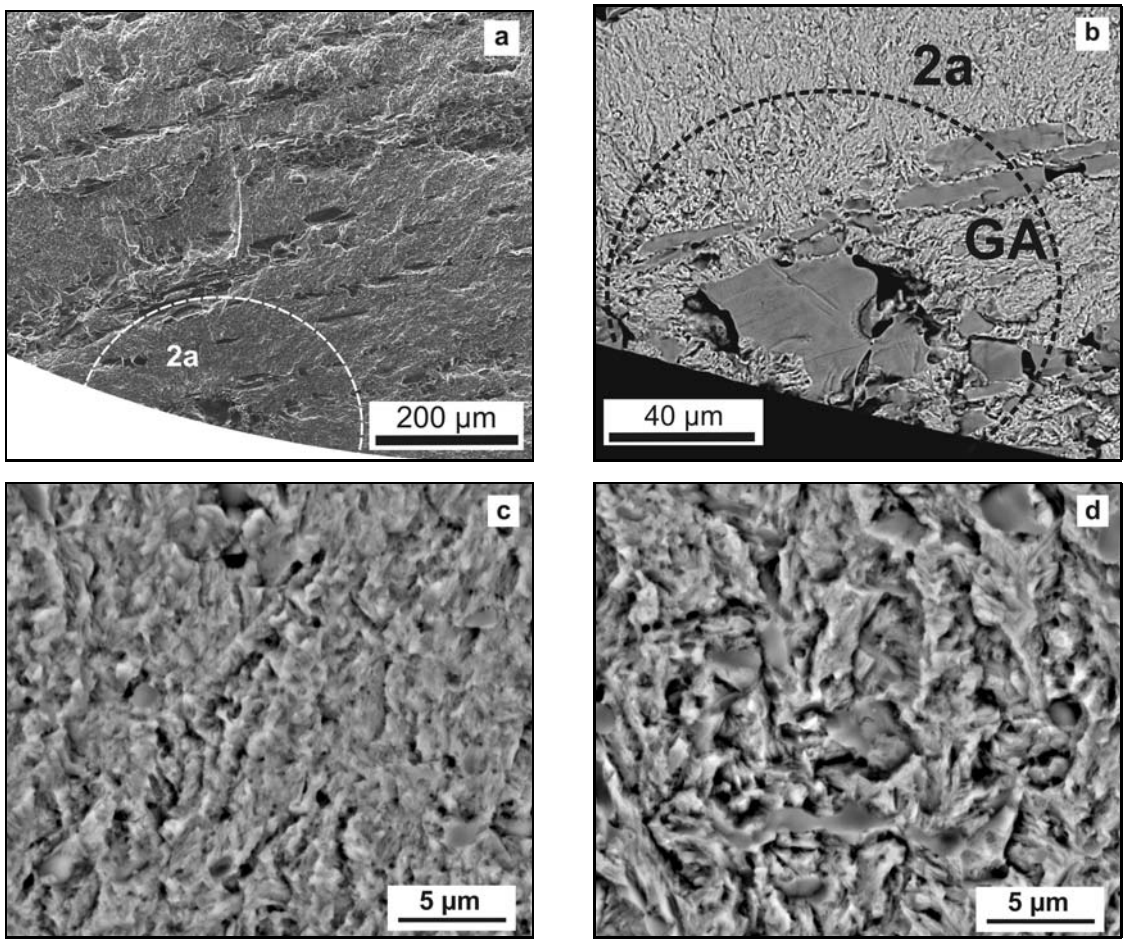

Fig. 7. Formation of granular area and subsequent area of short fatigue crack propagation ("2a") in AISI D2 type tool steel specimens failed after 2.4×10^7 cycles at 450 MPa; High magnification BSE image of (c) area "2a" and (d) of the granular area (GA).

minus carbide cluster size was zero, i.e. in this case the GA area is found only between the individual carbides forming the cluster but not around the cluster. Considering the fact that the GA size represents the critical crack length for a propagating short fatigue crack, this means that if this crack size can be reached by the size of the carbide cluster itself no formation of GA is required. This seemed to be the case for the higher stress amplitudes. However, at lower stress amplitudes the carbide clusters are not large enough in order to nucleate a short fatigue crack. Thus, the microcrack formation and coalescence occur until appropriate GA size is reached according to the Shiozawa [16] model described above. It is speculated that the formation of the granular area takes a rather long time period during the fatigue process, thus being decisive for fatigue life.

Interesting results were obtained when combining the two datasets for carbide cluster and GA sizes of K110TT and K110L specimens. Figure 8c presents the relationship with the applied stress amplitude.

Instead of showing a correlation with the applied stress amplitude, the radii of carbide clusters rather revealed two data sets – one for transversal samples (Fig. 8▲ – K110TT) and one for the longitudinal samples (Fig. 8Δ). Larger clusters (Fig. 8▲) were found in crack origins of K110TT specimens, which have been described above. In contrast, radii of carbide clusters observed in origins of K110L fractures (Fig. 8△) were not larger than 25 µm. This observation clearly underlines the material anisotropy, and corresponds also to the results of the metallographic investigations. In contrast to the carbide cluster size, the combined data of GA size (Fig. 8c●,○) could be correlated linearly to the applied stress amplitude: The lower the applied stress amplitude, the larger was the observed granular area, which supports the idea that the size of the GA represents the critical crack length for a propagating short fatigue crack. Interestingly, for K110L and LL specimens no fractures occurred below 400 MPa (Fig. 3), which was attributed to the smaller carbide cluster dimensions into that direction, as discussed above. Considering the data of Fig. 8c, it seems that the carbide clusters in K110L were not

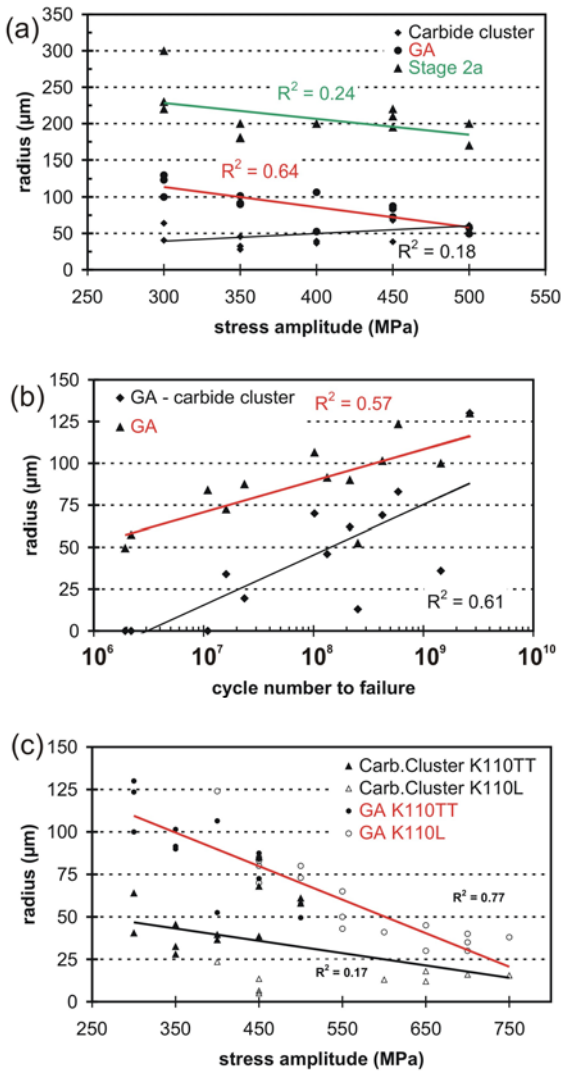

Fig. 8. Relationship of different zones of the fatigue process with: (a) the applied stress amplitude (K110TT specimens), (b) the cycle number to failure (K110TT), and (c) the applied stress amplitude for combined data set of K110TT and K110L specimens.

large enough to form appropriate sized GA at low stresses, or that the GA formation might take longer than 10^{10} cycles to attain the critical GA size. This further supports the hypothesis that most of fatigue life to failure is spent for the GA formation. In contrast, carbide clusters in longitudinal direction of the rolled steel (K110TT specimens) were large enough to form a granular area also below 400 MPa down to 300 MPa. Thus, K110TT samples failed at these lower stress amplitudes (Fig. 3). This further expresses the anisotropic fatigue behaviour of the studied AISI D2 type tool steel.

Summarizing, all the observations mentioned above support the significance of the GA formation for the fatigue process at low stress amplitudes in the gigacycle fatigue regime.

Furthermore, the authors recently determined stress intensity factor thresholds for the tool steel studied here through detailed fractographic evaluation [15]. Using the value obtained in that study [15], $\Delta K_{\text{carbide clusters}}$ (2.6 MPa $\sqrt{\text{m}}$), and the equation for surface cracks $\Delta K = 1.2584\ \sigma_a \sqrt{c}$ [15], where c represents half of the crack length – which is assumed to be equal to the radius of defect (here: carbide cluster) – provides an estimation for probable fatigue endurance strength at 10^{10} cycles of the material. Using the radius of largest primary carbide cluster (50 µm) observed in metallographic section (Table 2, bar B, longitudinal direction) give an estimate of the fatigue endurance strength of 290 MPa. If the largest cluster observed in fatigue failure origin of K110TT samples (90 µm) is used for the calculation, the fatigue endurance strength turned out to be 220 MPa. Both numerical results turned out to be rather good estimates for the fatigue endurance strength close to the experimentally obtained fatigue endurance strength after 10^{10} loading cycles which was about 250 MPa.

4. Conclusions

The presented work aimed to evaluate probable anisotropy of gigacycle fatigue of AISI D2 type (DIN Nr. 1.2379) wrought cold work tool steel loaded up to 10^{10} cycles by employing ultrasonic fatigue testing system (20 kHz, $R = -1$). Furthermore, the influence of the degree of deformation during hot working on the fatigue behaviour was also under investigation. The following important results were observed:

– The studied tool steel revealed a strong anisotropic fatigue behaviour. Specimens with their axis perpendicular to the rolling direction (K110TT) exhibited significantly lower fatigue strength within the entire cycle number range compared to samples with their axis in rolling direction (K110L,LL). At 10^{10} cycles the fatigue endurance strength of K110TT samples (250 MPa) was about 150 MPa lower than for K110L,LL samples (400 MPa).

– Crack initiation sites in all test series were closely arranged carbide particles (carbide clusters) or large primary carbides. They were located at/near the surface since there the stress concentration is highest due to superposition of the stress field of the defect particles and the free surface.

– The lower fatigue strength of K110TT specimens was directly attributed to the significantly larger carbide cluster sizes in transverse direction of the rolled steel bar. Also in the crack origins of K110TT fractures significantly larger carbide clusters were observed compared to that found in K110L,LL fracture origins, which explains the anisotropy of the fatigue behaviour of the studied tool steel.

– The degree of the deformation did not show an influence on the fatigue behaviour of the steel, at least parallel to the rolling direction. The specimens of test series K110L and LL – machined from bars with different diameters – failed within similar cycle number ranges and also the carbide clusters observed in the crack origins revealed similar sizes. This similarity was attributed to the hardly different sizes of carbides (clusters) observed in metallographic sections.

– The anisotropic fatigue behaviour of the material appeared also when comparing the fracture surfaces of K110TT and K110LL specimens. A very different macroscopic appearance was observed: In K110LL fractographs numerous cracks, found at the major part of the fracture surface, point back to the fatigue crack origin. K110TT fractures exhibited numerous cracks, oriented parallel to the primary carbide bands.

– However, despite this difference the fracture surfaces showed also similarities: Around the crack origin a granular area (GA) was formed, which, according to a model proposed by Shiozawa et al. [16], is generated by multiple microcrack formation and subsequent coalescence. Granular area sizes revealed strong relationship with the applied stress amplitude and the cycle number to failure. The GA was followed by a zone offering very flat surface morphology (Stage "2a"). These similarities suggest that the crack nucleating process and the first phases of crack propagation are rather similar for both material orientations, and that the anisotropic fatigue behaviour primarily is due to the different sizes of carbide clusters in the two orientations.

Acknowledgements

This project is supported by the Austrian Science Fund (FWF project number P17650-N02). Prof. E. Halwax of the Institute of Chemical Technologies and Analytics, Vienna University of Technology, is gratefully thanked for the accomplishment of XRD.

References

[1] PHADKE, V. B.—WISE, M. L. H.: Prakt. Metallogr., *20*, 1983, p. 621.
[2] BERNS, H.—TROJAHN, W.: VDI-Z, *127*, 1985, p. 889.
[3] BERNS, H.—LUEG, J.—TROJAHN, W.—WÄHLING, R.—WISELL, H.: Powder Metall. Int., *19*, 1987, p. 22.
[4] FUKAURA, K.—YOKOYAMA, Y.—YOKOI, D.—TSUJII, N.—ONO, K.: Met. Mat. Trans. A, *35A*, 2004, p. 1289.
[5] MARSONER, S.—EBNER, R.—LIEBFAHRT, W.—JEGLITSCH, F.: HTM, *57*, 2002, p. 283.
[6] MARSONER, S.—EBNER, R.—LIEBFAHRT, W.: BHM, *148*, 2003, p. 176.
[7] MEURLING, F.—MELANDER, A.—TIDESTEN, M.—WESTIN, L.: Int. J. Fatigue, *23*, 2001, p. 215.
[8] SOHAR, C. R.—BETZWAR-KOTAS, A.—GIERL, C.—WEISS, B.—DANNINGER, H.: Int. J. Fatigue, *30*, 2008, p. 1137.
[9] BERGER, C.—PYTTEL, B.—SCHWERDT, D.: In: Proceedings Werkstoffprüfung 2007. Eds.: Pohl, M. Bochum, Ruhr-Universität Bochum 2007, p. 1.
[10] FURUYA, Y.—MATSUOKA, S.—ABE, T.: Met. Mat. Trans. A, *35A*, 2004, p. 3737.
[11] TEMMEL, C.—KARLSSON, B.—INGESTEN, N.-G.: Met Mat Trans A, *37A*, 2006, p. 2995.
[12] KAYNAK, C.—ANKARA, A.—BAKER, T. J.: J. of Materials Science and Technology, *12*, 1996, p. 557.
[13] BORBÉLY, A.—MUGHRABI, H.—EISENMEIER, G.—HÖPPEL, H. W.: Int. J. Fracture, *115*, 2002, p. 227.
[14] MURAKAMI, Y.—NOMOTO, T.—UEDA, T.—MURAKAMI, Y.: Fract. Engng. Mater. Struct., *23*, 2000, p. 893.
[15] SOHAR, C. R.—BETZWAR-KOTAS, A.—GIERL, C.—WEISS, B.—DANNINGER, H.: Int. J. Fatigue, doi:10.1016/j.ijfatigue.2008.05.013.
[16] SHIOZAWA, K.—MORII, Y.—NISHINO, S.—LU, L.: Fract. Engng. Mater. Struct., *28*, 2006, p. 1521.